FULL PAPER

Sulfide Oxidation by Hydrogen Peroxide Catalyzed by Iron Complexes: Two Metal Centers Are Better Than One

Yasmina Mekmouche,[a] Helga Hummel,[a] Raymond Y. N. Ho,[b] Lawrence Que, Jr.,[b] Volker Schünemann,[c] Fabrice Thomas,[c] Alfred X. Trautwein,[c] Colette Lebrun,[d] Karine Gorgy,[e] Jean-Claude Leprêtre,[e] Marie-Noëlle Collomb,[e] Alain Deronzier,[e] Marc Fontecave,*[a] and Stéphane Ménage*[a]

Abstract: Peroxoiron species have been proposed to be involved in catalytic cycles of iron-dependent oxygenases and in some cases as the active intermediates during oxygen-transfer reactions. The catalytic properties of a mononuclear iron complex, $[Fe^{II}(pb)_2(CH_3CN)_2]$ (pb = (−)4,5-pinene-2,2′-bipyridine), have been compared to those of its related dinuclear analogue. Each system generates specific peroxo adducts, which are responsible for the

Keywords: bioinorganic chemistry · enantioselective catalysis · hydrogen peroxide · iron · peroxoiron adducts

oxidation of sulfides to sulfoxides. The dinuclear catalyst was found to be more reactive and (enantio)selective than its mononuclear counterpart, suggesting that a second metal site affords specific advantages for stereoselective catalysis. These results might help for the design of future enantioselective iron catalysts.

Introduction

Non-heme diiron(III) complexes are of great interest as chemical models for a particular class of enzymes, the so-called diiron–oxo proteins. These enzymes contain an active site consisting of two ferric ions linked by an oxygen atom and one or two carboxylate bridges in their resting state.[1] Methane monooxygenase (MMO), isolated from methanotrophic organisms, catalyzes the transformation of methane into methanol by using molecular oxygen as the oxidant in the presence of a source of electrons.[2, 3] Furthermore, hydrogen peroxide can also be used as the oxidant, with no need for a reducing agent.[4] Enzymes belonging to this class of proteins catalyze a great variety of reactions: toluene 2- or 4-monooxygenase (aromatic hydroxylation of toluene),[5] alkene monooxygenase (epoxidation),[6] membrane stearoyl-CoA Δ^9 desaturase (incorporation of double bonds).[7] The enzymatic mechanism of MMO and related enzymes has been partially elucidated by stopped-flow kinetic and rapid-freeze-quench spectroscopic studies. First, dioxygen binds to the diferrous active site leading to the first intermediate, compound **P**, proposed to be a (μ-peroxo)diferric center.[8, 2a] Compound **P** decays to compound **Q**, identified as a coupled Fe_2^{IV} unit.[9] It has been proposed that the reaction products are derived from the two-electron oxidation of the substrate by compound **Q**. In one case, compound **P** was proposed to be the active species in olefin oxidation by a direct oxygen transfer.[10]

The discovery that a non-heme iron biocatalyst can perform selective oxidations by using hydrogen peroxide as an oxidant has stimulated research in this field. There has been some success with synthetic diiron catalysts, the molecular structures of which reproduce the active site of MMO.[11] Other oxidants such as alkyl hydroperoxides and peracids were also used.[12] On the other hand, mononuclear iron complexes were also found to be efficient catalysts[13] raising the question of why in biological systems is a dinuclear center often preferred.

[a] Prof. M. Fontecave, Dr. S. Ménage, Y. Mekmouche, Dr. H. Hummel
Laboratoire de Chimie et Biochimie des Centres Rédox Biologiques
Université Joseph Fourier/DBMS/CEA, UMR CNRS 5047 Grenoble
17 rue des Martyrs, 38054 Grenoble Cédex 9 (France)
Fax: (+33) 4-38-78-91-24
E-mail: smenage@cea.fr

[b] Dr. R. Y. N. Ho, Prof. L. Que, Jr.
Department of Chemistry and Center for Metals in Biocatalysis
University of Minnesota, Minneapolis, Minnesota 55455 (USA)

[c] Dr. V. Schünemann, Dr. F. Thomas, Prof. A. X. Trautwein
Institut für Physik Medizinische Universität
Ratzeburger Allee 160, D-23538 Lübeck (Germany)

[d] C. Lebrun
Service de Chimie Inorganique et Biologique
DRFMC CEA-Grenoble (France)

[e] Dr. K. Gorgy, Dr. J.-C. Leprêtre, Dr. M.-N. Collomb, Dr. A. Deronzier
Laboratoire d'Electrochimie Organique et de Photochimie Rédox
CNRS UMR 5630, 38041 Grenoble (France)

Supporting information for this article is available on the WWW under http://wiley-vch.de/home/chemistry/ or from the author: 4.2 K Mössbauer spectrum of 1 mM Fe ^{57}Fe-complex **1** at $B_{ext} = 20$ mT.

The catalytic mechanism of model systems for alkane oxidation has been partly elucidated. With alkyl hydroperoxides activation of the oxidant occurs by coordination to iron. During the reaction dinuclear complexes are converted into mononuclear ferric alkylperoxo species, which undergo homolytic cleavage of the O–O bond.[14] The resulting alkoxy radicals abstract the hydrogen atom from the substrate. The free substrate radical then reacts with dioxygen to produce alcohols and ketones (autoxidation reaction), but, under certain conditions, may react with the high-valent Fe^{IV} intermediate, produced during the O–O cleavage reaction.[14] In contrast, there is some evidence that metal-based mechanisms may occur when H_2O_2 is used as the oxidant. As a matter of fact, oxidations can be made stereoselective, thus excluding pure free-radical chemistry.[15]

We have recently shown that a dinuclear iron complex $[Fe_2O(pb)_4(H_2O)_2](ClO_4)_4$ (**1**), containing the chiral ligand pb (pb = (−)4,5-pinene-2,2′-bipyridine),[16] was able to catalyze the enantioselective sulfide oxidation with H_2O_2 as the oxidant. The active species was shown to be the peroxo adduct of **1**, based on kinetic and spectroscopic studies, and the reaction proceeded through the nucleophilic attack of the sulfide to the iron peroxide intermediate.[17]

We found this selective sulfide oxidation to be a suitable reaction probe to compare the dinuclear complex **1** and the corresponding mononuclear analogue, formulated as $[Fe(pb)_2(CH_3CN)_2](ClO_4)_2$ (**2**), in order to determine whether a dinuclear structure may provide specific and significant advantages over a mononuclear one for controlling oxidation reactions (Scheme 1). Here, we report the characterization of
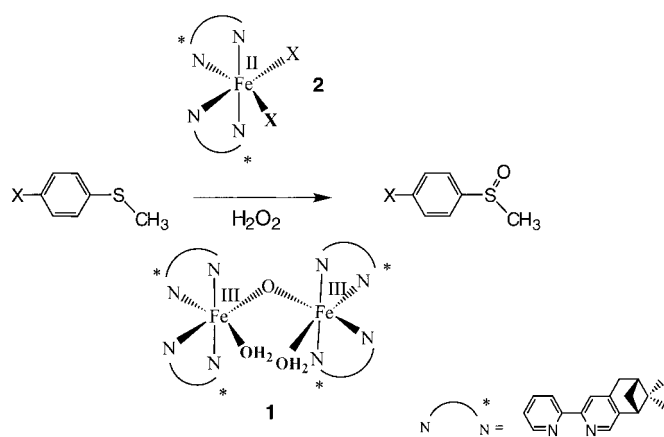
Scheme 1. Oxidation of sulfide catalyzed by complex **1** or **2**.

complex **2** and its catalytic activity during oxidation of sulfides by H_2O_2. The corresponding ferric peroxide adduct, which is the active oxidizing species, has been observed and characterized in solution. Its reactivity has also been compared to that of the diferric peroxide complex, derived from complex **1**, in terms of the enantioselectivity it can provide. We demonstrate that, at least in the case of sulfoxidation, a dinuclear unit affords a better selectivity than a mononuclear one. In addition, we confirm that peroxoiron species are capable of direct oxygen transfer, with no need for O–O cleavage as a prerequisite. On the whole, this study affords new insights for the design of more efficient enantioselective catalysts.

Experimental Section

Materials: Most of the reagents were of the best commercial grade available and were used without further purification. Naphthyl methyl sulfide was prepared from the corresponding aryl thiol by alkylation with 1,8-diazabicyclo[5.4.0]undec-7-ene (DBU) and iodomethane[18] in toluene. Sulfoxides were prepared from the parent sulfide by sodium metaperiodate oxidation in methanol.[19] All these compounds were isolated by column chromatography on silica gel. The purity of the compounds was checked by GC, and they were identified by ^{1}H and ^{13}C NMR spectroscopy. The concentration of H_2O_2 was determined by iodometric titration.

Synthesis of complexes: Dinuclear complex **1** was synthesized as previously described,[17] but all attempts to prepare the mononuclear ferric complex $[Fe^{III}(pb)_2(X)_2]^{3+}$ (X = CH_3CN or H_2O) during the reaction of ferric salts with the pb ligand failed because of the propensity of the reactants to generate a dinuclear complex. However, a mononuclear ferrous complex, formulated as $[Fe^{II}(pb)_2(CH_3CN)_2](ClO_4)_2$ (**2**), could be obtained by the reduction of complex **1**. A solution of **2** in CH_3CN was prepared as follows: Complex **1** (10 mg) was dissolved in CH_3CN (6 mL) in a glove box and ascorbic acid (2 mg) was added at room temperature. The excess reducing agent was removed by filtration and the orange solution used directly for reactivity and spectroscopic studies. The solution no longer gave rise to an absorbance at 610 nm, in accordance with the disappearance of complex **1**. ^{1}H NMR (CD$_3$CN): δ = 9.1 (Hαpy), 8.0 (t), 3.4 (m), 2.75 (s), 2.33 (s), 1.34 (s), 0.65 (s); UV/Vis (CH$_3$CN): λ_{max} (ε) = 470 nm (4000 mol^{-1} dm^3 cm^{-1}).

Mössbauer samples: The [57]Fe complex **1** sample was prepared as follows: [57]Fe$_2$O$_3$ (9 mg) was placed in a 5 mL vial and HClO$_4$ (36 μL) was added. The reaction mixture was stirred and heated at 150 °C for two days. During this period three additions of HClO$_4$ and water were made. When the solution was transparent it was concentrated until a white powder appeared, but it was not allowed to reach dryness. The Fe(ClO$_4$)$_3$ salt was used directly for complex synthesis (see Ref. [17]). [*CAUTION: perchlorate salts are potentially explosive and should be used with care and appropriate safety precautions.*] [57]Fe complex **2** was obtained by chemical reduction of a solution containing [57]Fe complex **1** (see above). For all of the Mössbauer samples, an EPR and a UV/Vis spectrum were recorded.

Physical methods: 300 MHz ^{1}H NMR spectra were recorded on a DPX 300 Brüker spectrometer. Visible absorption spectra were recorded on a Varian Cary1Bio and HP 8453 diode-array spectrophotometers. Gas chromatography (GC) was performed on a Perkin–Elmer Autosystem instrument connected to a PE NELSON 1022 integrator with a FID detector, using a SE 30 column. Resonance Raman spectra were collected on an Acton AM-506 spectrometer (2400-groove grating) using a Kaiser Optical holographic super-notch filter with a Princeton Instruments liquid N$_2$-cooled (LN-1100PB) CCD detector with 4 cm^{-1} spectral resolution. Spectra were obtained using back-scattering geometry on liquid N$_2$-frozen samples using 632.8 or 578.0 nm excitation from a Spectra Physics 2030-15 argon-ion laser and a 375 B CW dye (Rhodium 6 G) laser. Raman frequencies were referenced to indene. Mössbauer spectra were recorded on 400 μL cups containing the complex (1 mM) with a conventional constant acceleration spectrometer by using a [57]Co source in a Rh matrix (1.85 Gbq). The low-field measurements were performed at 4.2 K by using a bath cryostat (Oxford Instruments) with a magnet mounted outside the cryostat producing a field of 2 mT perpendicular to the γ beam. Measurements at 7 T perpendicular and parallel to the γ beam were performed with a cryostat equipped with a superconducting magnet (Oxford Instruments). The spectra were analyzed assuming Lorentzian line shape and, in the case of a magnetically split pattern, with the Spin Hamiltonian formalism.[20] The isomer shifts are quoted relative to α-Fe at room temperature.

ESI-MS spectra were obtained on an LCQ ion-trap spectrometer by using a method developed previously.[21] Cyclic voltammetry and controlled-potential electrolysis experiments were performed using a PAR model 273 potentiostat/galvanostat, a PAR model 175 universal programmer, and a PAR model 179 digital coulometer. Potentials are referenced to an Ag/10 mM AgNO$_3$ electrode in CH$_3$CN + 0.1 M TBAP. The working electrodes were platinum and vitreous carbon discs.

Catalytic oxidation of sulfides by hydrogen peroxide: Standard conditions were as follows: Complex **1** or **2** (7.0 μmol) was dissolved in CH$_3$CN containing the sulfide (4.2 mmol) under an atmosphere of argon at 0 °C (final volume: 10 mL). The reaction was started by adding H$_2$O$_2$ (70 μmol;

ratio of complex **2**:sulfide:$H_2O_2 = 1:600:10$). After stirring for 10 minutes, an internal standard (20 µmol; benzophenone or fluorenone) was added to the reaction mixture, and the organic products were quantified by GC. Unambiguous identification of the products was made by comparison with pure compounds, which were either prepared independently or commercially available. The *ee* was determined as previously described.[17]

Kinetic studies: Kinetic experiments were carried out in CH_3CN at 20 °C. The reaction mixture, placed in a 0.1 cm optical path UV cell, contained complex **2**, methyl phenyl sulfide, and hydrogen peroxide in a total volume of 160 µL. Reactions were initiated after the addition of H_2O_2 and followed by the variation of the difference in absorption at a fixed wavelength, λ, between the sulfide and the corresponding sulfoxide. Initial rates were calculated by using the difference of molar extinction coefficients ($\Delta\varepsilon$) between the sulfides and the corresponding sulfoxides.[17]

Reactivity of the hydroperoxo adduct of complex 2: The peroxo adduct was generated at 20 °C by mixing 0.15 mL (13.5 mM) of hydrogen peroxide and 0.25 mL (0.810 mM) of complex **2** in CH_3CN (final volume: 1 mL). Its decomposition in the presence of increasing amounts of methyl phenyl sulfide (0–100 mM) was monitored by the decay of the absorbance at 700 nm as a function of time. This was fitted to a pseudo first-order kinetic law. The peroxoiron species was quantified by using an approximate value of 2000 for the molar absorption coefficient at 560 nm. This value is in the range of coefficients for hydroperoxoiron complexes previously reported.[22]

Results

Synthesis and characterization of [Fe(pb)₂(CH₃CN)₂](ClO₄)₂ (2): A mononuclear low-spin ferrous complex, formulated as $[Fe(pb)_2(CH_3CN)_2](ClO_4)_2$ (**2**), can be prepared in CH_3CN under anaerobic conditions from complex **1** either electrochemically, by exhaustive controlled potential electrolysis at $E = 0$ V,[23a] or chemically, using ascorbic acid (two equivalents) as the reductant.[23b]

The UV/Vis spectrum of complex **2** displayed an intense transition at 470 nm ($\varepsilon = 4000\ mol^{-1}\ dm^3\ cm^{-1}$), assigned to metal-to-ligand charge transfer.[24] The extinction coefficient was calculated by using the concentration of **2** determined by Mössbauer spectroscopy (vide infra) and confirmed by using the one issued from the electrochemical synthesis. The ^1H NMR spectrum of the solution showed resonances mainly in the diamagnetic region, indicating that the majority of the iron centers are in the low-spin ferrous state. The resonances of the pyridine protons differed from those of the free ligand. A large broadening for the α protons at $\delta = 9.1$ was observed, due to the proximity of the ferrous ion. Resonances above $\delta = 10$ were attributed to an impurity, most probably a high-spin ferrous complex also found in the Mössbauer spectra of solutions of complex **2** (see below).

The Mössbauer spectrum of a solution of the ^{57}Fe-enriched complex **1** after reduction with ascorbic acid is shown in Figure 1. The spectrum, taken at 4.2 K, consists of three doublets: The minor doublet 1 ($\delta = 0.48\ mms^{-1}$; $\Delta E_Q = 1.53\ mms^{-1}$; 12 % of the total area) can be attributed to a (μ-oxo)diferric species related to complex **1** from a comparison with the spectrum of a sample containing the pure complex **1** (see Supporting Information). Doublet 2, with an isomer shift of $\delta = 0.42\ mms^{-1}$ and a quadrupole splitting of $\Delta E_Q = 0.56\ mms^{-1}$, corresponds to complex **2** and represents 76 % of the total area of the spectrum. This major component exhibits no magnetic splitting at 4.2 K, which is consistent with
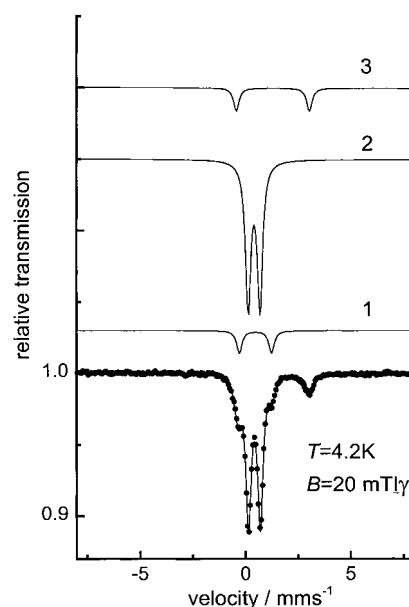

Figure 1. Mössbauer spectrum of complex **2** after reduction of complex **1** with ascorbic acid obtained at 4.2 K and $B = 20$ mT perpendicular to the γ-beam. The solid lines are Lorentz fits with the following parameters: Component 1 represents residual complex **1** ($\delta = 0.48\ mms^{-1}$; $\Delta E_Q = 1.53\ mms^{-1}$, rel. area 12 %); Component 2 represents the ferrous low-spin complex **2** ($\delta = 0.42\ mms^{-1}$, $\Delta E_Q = 0.56\ mms^{-1}$, rel. area 76 %); Component 3 is a ferrous high-spin impurity ($\delta = 1.32\ mms^{-1}$; $\Delta E_Q = 3.48\ mms^{-1}$; rel. area 12 %). The line width has been taken as $\Gamma = 0.30\ mms^{-1}$ for all three subspectra.

a diamagnetic state of the iron site. Both the relatively low quadrupole splitting and the value of the isomer shift are consistent with a low-spin ($S = 0$) ferrous iron center, the presence of which has also been indicated by NMR spectroscopy (see above). A third component (doublet 3, 12 % of the total area) exhibits $\delta = 1.32\ mms^{-1}$ and $\Delta E_Q = 3.48\ mms^{-1}$. These parameters are typical for a high-spin ($S = 2$) ferrous complex, the structure of which remains unknown.
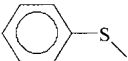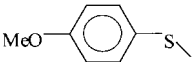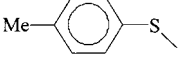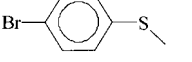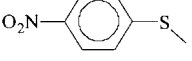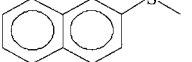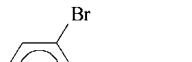
Complex **2** was quite stable in aerated CH_3CN solution ($t_{1/2} = 2$ h) and mainly decomposed into $[Fe(pb)_3]^{2+}$, characterized by an absorption in the visible region ($\lambda\ (\varepsilon) = 521$ nm (8500 $mol^{-1}\ dm^3\ cm^{-1}$)). Complex **2** could be formulated on the basis of its electrospray mass spectrum, which exhibited only four peaks at m/z (%): 278 (90), 298.5 (100), 655 (30), and 403 (30). These features correspond to the $[Fe(pb)_2]^{2+}$, $[Fe(pb)_2(CH_3CN)]^{2+}$, $[Fe(pb)_2(ClO_4)]^+$ and $[Fe(pb)_3]^{2+}$ ions, respectively, and all show the correct isotopic distribution patterns. The observation of the m/z 298.5 feature suggests that CH_3CN is very likely to be a ligand.

From all these results, complex **2** can be best described as a mononuclear diamagnetic low-spin ferrous complex with two pb and two CH_3CN ligands, analogous to several other low-spin ferrous complexes with CH_3CN and nitrogen ligands.[24, 25]

We noted that from one preparation to another, complex **2** consistently represented 80–90 % of the species present in solution based on UV/Vis titration.

Sulfide oxidation catalyzed by complex 2 and kinetic studies: As shown in Table 1, solutions of complex **2** in CH_3CN were

Table 1. Oxidation of prochiral sulfides by hydrogen peroxide catalyzed by **1** and **2**.[a]

Sulfide	ee [%] (enantiomer)		Yield[d] [%]	
	1[b]	**2**[c]	**1**[b]	**2**[c]
(phenyl)–S–CH3	21 (R)	5 (S)	90	20
+ 2 equiv Cl−[e]	0		–	
+ 0.3 equiv Cl−		5 (S)		20
MeO–(phenyl)–S–CH3	11 (R)	5 (R)	70	5
Me–(phenyl)–S–CH3	28 (R)	0	68	23
Br–(phenyl)–S–CH3	40 (R)	5 (S)	90	24
O2N–(phenyl)–S–CH3	4 (R)	0	45	48
(naphthyl)–S–CH3	40 (R)	0	80	6
(2-Br-phenyl)–S–CH3	26 (R)	0 (S)	80	10

[a] Experimental conditions: [complex] = 0.7 mM; ratio complex/sulfide/oxidant = 1:600:10, solvent CH3CN, room temperature. [b] Ref. [17]. [c] This work. [d] Yield based on the oxidant after 15 minutes of reaction. [e] Chloride equivalents based on complex **1** or **2** concentration.

able to catalyze the oxidation of aryl sulfides to sulfoxides with hydrogen peroxide as the oxidant at room temperature under argon. In these experiments, solutions of complex **2** were chosen so that complex **2** represented 90 % of the total iron based on UV/Vis spectroscopy and no oxidation could be observed in the absence of the iron complex. The ligand in combination with H_2O_2 was ineffective as well. We thus attribute the observed catalytic effect to complex **2** (see Discussion). With a 1:10 Fe/H_2O_2 ratio ([Fe] = 0.7 mM), yields after 15 minutes reaction ranged from 20–50 % with respect to the oxidant, with higher yields being obtained when methyl 4-nitro-phenyl sulfide was used as a substrate. Due to the instability of complex **2** in other solvents, solvent effects on the reaction could not be studied. In contrast, complex **1**, whose catalytic activities are displayed in Table 1 for comparison, gave reaction yields in the 50–90 % range (5–9 catalytic cycles).[17]

Furthermore, reactions catalyzed by complex **2** were essentially stereorandom. The highest ee value was 10 %, whereas it was 40 % with complex **1**. With almost all substrates the ee value was much higher when complex **1** was used as the catalyst; ee is not sensitive to the nature of the substituents on the phenyl ring of the methyl phenyl sulfide (Table 1).

Since an analogue of complex **1** was present as a contaminant in solution, shown spectroscopically, we checked whether it might contribute to the oxidation reaction. The activity of complex **1** is fully inhibited by the addition of two equivalents of chloride (Table 1), as the result of chloride coordination to the sixth position of the iron coordination

sphere. This a general trend of bipy- and phen-coordinated diferric complexes.[26] In a control experiment using ¹H NMR spectroscopy, we checked that Cl⁻ was ligated to complex **1**. Accordingly, the proton resonances of complex **1** were shifted and the peak pattern in the 20–10 ppm region was modified.[26] When a solution of complex **2**, supplemented with a slight excess of chloride with regard to the (μ-oxo) diferric contaminant, was assayed for catalytic activity during oxidation of methyl phenyl sulfide under standard conditions, the corresponding sulfoxide was formed with the same yield and ee as in the absence of Cl⁻. We thus assume that the contaminating dinuclear ferric species was not contributing significantly to the reaction catalyzed by the solution of complex **2**.

The initial rate of methyl phenyl sulfide oxidation was determined by UV spectrophotometry ($\lambda = 254$ nm) at 20 °C from the formation of the sulfoxide during the first 20 s. Since the highest accessible concentration of sulfide was about 1.25 mM, a catalyst concentration of 0.05 mM was used. In Figure 2 (top), the initial rate of the reaction was plotted as a
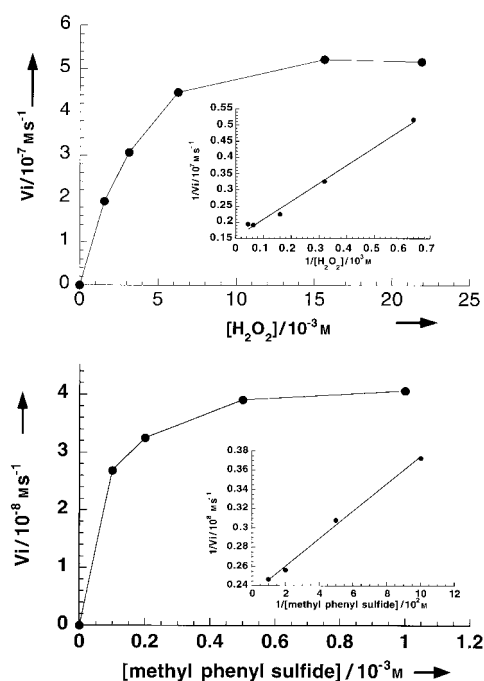
Figure 2. Initial rate of methyl phenyl sulfoxide formation as a function of hydrogen peroxide (top) and substrate (bottom) concentrations in CH3CN at 20 °C. Experimental conditions: [**2**] = 5 × 10⁻⁵ M; **2**/methyl phenyl sulfide: 1/25 (top); [**2**] = 1 × 10⁻⁵ M; **2**/hydrogen peroxide: 1/50 (bottom). Inset: reciprocal plots of the observed initial rates as a function of hydrogen peroxide (top) and substrate (bottom) concentrations.

function of H_2O_2 concentration. The observed saturation kinetics and the fact that the initial rates followed typical Michaelis–Menten kinetics most likely imply a kinetic scheme in which the H_2O_2 binds to complex **2** to generate an active oxidizing intermediate.

The same kinetic analysis was applied to the dependence of the initial rate of the reaction on the concentration of the sulfide substrate, with H_2O_2 kept at 0.5 mM (Figure 2, bottom). Again, a saturation behavior with respect to sulfide concen-

tration was observed. A double reciprocal plot of the results displays a straight line, indicating that the sulfide is also bound to the complex during the reaction. Since these experiments could not be carried out in the presence of a saturating concentration of the fixed substrate, accurate K_m values could not be determined.

The initial rates of the oxidation were found to be dependent on the *p*-substitution of the aryl methyl sulfides, but no correlation could be observed with Hammet parameters in contrast to the σ_p correlation observed with complex **1**.[17]

Characterization of a peroxoiron complex formed during reaction of complex 2 with H$_2$O$_2$: Addition of H$_2$O$_2$ to a CH$_3$CN solution of **2** (complex **2** accounting for about 90% of the total iron as titrated by UV/Vis spectroscopy) resulted in a transient color change from orange to brown. Following the reaction by UV/Vis spectroscopy at $-20\,^\circ$C allowed us to stabilize the transient chromophore characterized by a broad band at around 560 nm ($\varepsilon = 2000\ \mathrm{mol^{-1}\,dm^3\,cm^{-1}}$ based on iron titration by Mössbauer) that appeared at the expense of the absorption at 470 nm characteristic of complex **2** (Figure 3). Under these conditions, 50 equivalents of oxidant
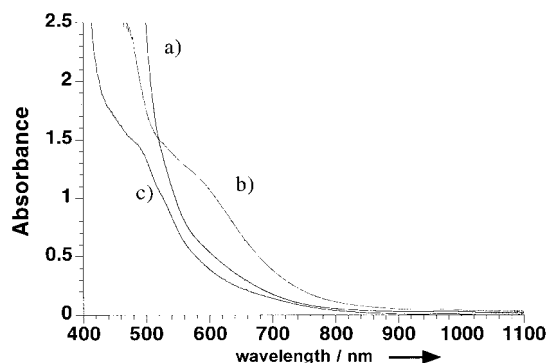

Figure 3. UV/Vis spectra of 2.1 mM complex **2** with 50 equivalents of H$_2$O$_2$: a) complex **2**; b) **2** + H$_2$O$_2$ at the maximum 570 nm absorbance; c) after decomposition at room temperature.

elicited the largest amount of this new chromophore. Lowering the temperature, using different solvents such as CH$_2$Cl$_2$ or ethanol, or adding triethylamine resulted in lower amounts of the 560 nm-absorbing species.

After freezing in liquid N$_2$, the 560 nm-absorbing solution exhibited resonance-enhanced Raman features at 811 and 623 cm^{-1} upon excitation at 578 nm (Figure 4). The most intense and best resolved Raman spectrum was obtained in
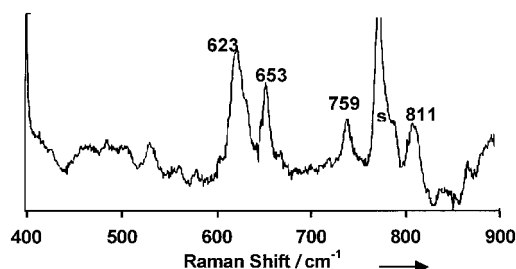

Figure 4. Resonance-enhanced Raman spectrum of 5 mM complex **2**/H$_2$O$_2$ adduct ($\lambda_{\mathrm{exc}} = 578.0$ nm; CH$_3$CN:THF 9:1).

CH$_3$CN/THF (90:10 v/v) to minimize the fluorescence background of the sample. The observed vibrations were attributed to O−O and Fe−O vibrations, respectively, similar to those previously reported for mononuclear low-spin iron complexes with an η^1-peroxo ligand.[22] These features are clearly distinct from those of the peroxodiiron complexes derived from complex **1**.[17] Furthermore, the absorbance at 560 nm could be correlated with the intensity of an axial X-band EPR signal with $g_\perp = 2.18$ and $g_\parallel = 1.97$, characteristic of a low-spin ferric species (Figure 5).
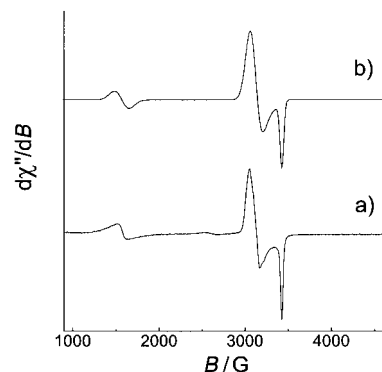

Figure 5. a) EPR spectrum of 2.1 mM complex **2** with 50 equivalents of H$_2$O$_2$ at the maximum at 570 nm ($T = 10$ K, microwave power 0.1 mW, frequency: 9.4 GHz; modulation 10 Gauss); b) Simulation assuming Lorentzian line shape with $g_x = 1.97$ and $g_y = g_z = 2.18$ and the linewidths $\Gamma_x = 5$ mT and $\Gamma_y = \Gamma_z = 15$ mT. The $g = 4.3$ signal represents 7% of the total spins taking into account the Aasa–Vånngard factors[37] and assuming equal population of the three Kramers doublets.

Low- and high-field Mössbauer spectra of a solution of **2**/H$_2$O$_2$ (50 equivalents) obtained at 4.2 K are shown in Figure 6a and b. The spectra contained four components, the parameters of which are listed in Table 2. The diamagnetic component 1 represents 30% of the total area and has $\delta = 0.48$ mms^{-1} and $\Delta E_Q = (-)1.53$ mms^{-1}. These parameters are in the range of those for the μ-oxo dinuclear complexes such as complex **1**. The diamagnetic component 2 exhibits Mössbauer parameters identical to those of unreacted complex **2** (25% of the total iron). There is also a high-spin ferric impurity (component 3) evident from the high-field spectra. Since the EPR spectrum also shows the presence of 7% of a high-spin ferric signal, we used the rhombicity parameter ($E/D = 0.33$) from the EPR spectrum and a relatively small zero-field splitting $D = 0.5$ cm^{-1}[27] in order to simulate the contribution of this minor impurity. Component 4, the magnetic structure of which did not disappear even at 77 K (data not shown), exhibits 38% of the total area and was found to correlate with the $S = 1/2$ signal observed in the EPR spectrum (spin quantification yielded 40%). Since this signal was found to be transient, we tentatively assigned it to the paramagnetic mononuclear low-spin peroxoiron(III) species. From these data, it is clear that the major species formed is a low-spin peroxoiron(III) species that is responsible for the features in the Raman and EPR spectra. These data have been reproduced with two different samples.

According to Oosterhuis, Lang[28] and Taylor[29] it is possible to calculate the magnetic hyperfine coupling tensor $\tilde{A}$ from
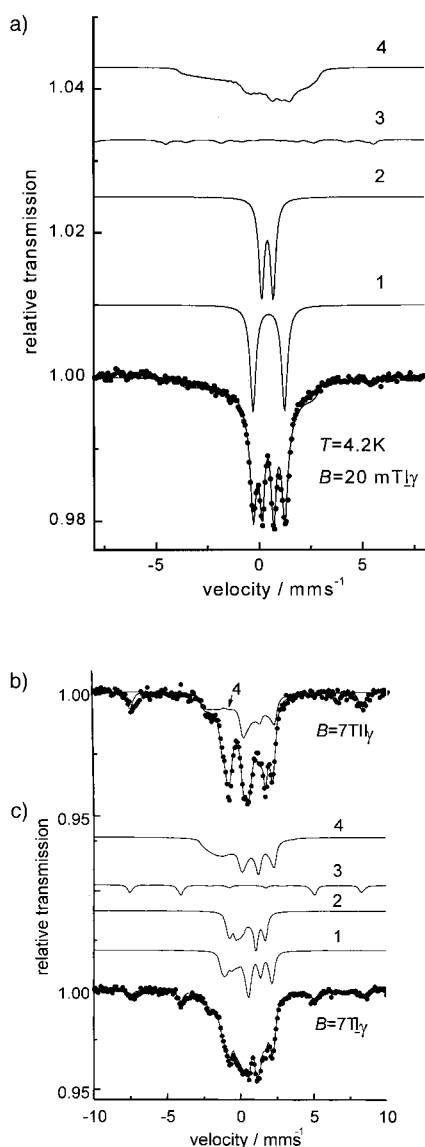
Figure 6. Mössbauer spectra of 2.1 mM complex **2** with 50 equivalents of H_2O_2 at the maximum 570 nm absorbance obtained at 4.2 K and a) $B = 20$ mT perpendicular to the γ-beam; b) $B = 7$ T parallel to the γ-beam; c) $B = 7$ T perpendicular to the γ-beam. The solid lines are simulated by the spin-Hamiltonian formalism with the parameters listed in Table 2. For clarity only subspectrum 4 is indicated in Figure 6b.

the **g** tensor of a low-spin ferric center in a six-coordinate environment. However, information about the orientation of the **g** tensor with respect to the molecular frame cannot be provided by Mössbauer spectroscopy thus far. In the case of

activated bleomycin, the only mononuclear low-spin peroxoiron(III) species investigated by Mössbauer spectroscopy, Burger et al. quoted the lowest **g** value to be g_{xx} (Table 3).[30]

Table 3. Mössbauer parameters of complex **2**/H_2O_2 and those of activated bleomycin.

| | **2**/H_2O_2[a] | | activated bleomycin[31] | |
	Experiment	Theory	Experiment	Theory
g_x	1.97	1.97	1.94	1.94
g_y	2.18	2.18	2.17	2.18
g_z	2.18	2.18	2.26	2.26
$A_{xx}/g_n\mu_n$ [T]	−40.	−52.3	48 ± 2	−48
$A_{xx}/g_n\mu_n$ [T]	−8	+5.4	+5	+7
$A_{xx}/g_n\mu_n$ [T]	+5	+5.4	+5	+13
ΔE_Q [mm s^{-1}][b]	1.71		3.0 ± 0.2	
δ [mm s^{-1}]	0.23		0.10 ± 0.07	
η	−3	–	+3	
Γ [mm s^{-1}]	0.30		–	

[a] This study. [b] The coordinate system of the efg (x',y',z') is often chosen such that $|V_{z'z'}| > |V_{y'y'}| > |V_{x'x'}|$. The Mössbauer parameters quoted in this coordinate system change for the peroxoiron(III) complex of this study to $\eta' = 0$, $\beta' = 90°$ and $\Delta E_Q' = -1.7$ mms^{-1}. Those for activated Fe–Bleomycin change to $\eta' = 0$, $\alpha' = 90°$, $\beta' = 90°$ and $\Delta E_Q' = -3$ mms^{-1}. α and β are the Euler angles defined in the usual manner.

Accordingly, we chose $g = (1.94, 2.18, 2.18)$. The resulting hyperfine coupling tensor $\tilde{A}/g_N\mu_N = (-52, 5.0, 5.0)$ T was then used as a starting parameter for the analysis of the spectra shown in Figure 6. The best fit of the experimental data for the low-spin peroxoiron(III) species was achieved with $\delta = 0.23$ mms^{-1}, $\Delta E_Q = 1.71$ mms^{-1}, $\eta = -3$, and $\tilde{A}/g_N\mu_N = (-40, -8, +5)$ T. As in the case of the activated Fe–Bleomycin complex, the magnetic splitting of the peroxo species is determined by the magnitude of the largest component of the **A** tensor, which we have chosen to be A_{xx}. Variation of A_{yy} influences the pattern in the middle of the Mössbauer pattern, but the spectrum is not very sensitive towards changes of A_{zz}. Our value of $|A_{xx}| = 40$ T is somewhat lower than that of activated Fe–Bleomycin ($|A_{xx}| = 48$ T), but one has to keep in mind that the quadrupole splitting for complex **2**/H_2O_2 is approximately only half that for Fe–Bleomycin (see Table 3). The isomer shift of 0.23 mms^{-1} for this species is significantly lower than the values reported in the literature for (μ-peroxo)diiron(III) complexes (typically about 0.54 mms^{-1}). However these last complexes consist of antiferromagnetically coupled high-spin ferric ions,[31] while low-spin ferric complexes are expected to have a much lower isomer shift.[32]

Finally, the solution containing the transient species could also be analyzed by ESI-MS. The spectrum contained new peaks with m/z (%): 294 (30) in the positive mode and m/z (%): 885 (100) in the negative mode, which may be assigned to the fragments [Fe(pb)$_2$(OOH)]$^{2+}$ (Figure 7) and [Fe(pb)$_2$(OOH)(ClO$_4$)$_3$]$^-$, respectively; the corresponding isotopic patterns of these ions fully agreed with those calculated for the given formulations. These fragments were absent in the starting and the
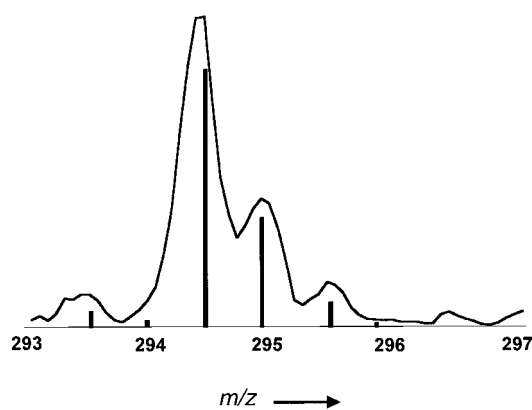
Table 2. Mössbauer parameters obtained from the spin-Hamiltonian simulations shown in Figure 6.

Subspectra[a]	S	**g**	δ [mms^{-1}]	ΔE_Q [mms^{-1}]	η	$\tilde{A}/g_N\mu_N$ [T]	rel. area [%]
1	0		0.48	−1.53	0.4		30
2	0		0.42	−0.56	0		25
3	5/2[b]	(2.0, 2.0, 2.0)	0.41	0.50	0	(−22.5, −22.5, −22.5)	7
4	1/2	(1.97, 2.18, 2.18)	0.23	1.71	−3	(−40, −8, +5)	38

[a] All components were simulated with a line width of $\Gamma = 0.3$ mms^{-1}. [b] For the simulation of the S = 5/2 species the rhombicity parameter $E/D = 0.33$ (from EPR) and a zero-field splitting of $D = 0.5$ cm^{-1} was used.[27]

Figure 7. ESI-MS fragment of $[Fe(OOH)(pb)_2]^{2+}$ and its calculated isotopic pattern.

final solution. No fragment ion corresponding to a dinuclear peroxoiron(III) adduct could be observed under these conditions, in agreement with the absence of the corresponding characteristic features in the Raman resonance and Mössbauer spectra.[33] Upon raising the temperature, the absorption band at 560 nm disappeared together with all the corresponding EPR, Mössbauer, and ESI-MS signals.

Therefore, we conclude that the addition of H_2O_2 to complex **2** at low temperature causes the formation of an unstable mononuclear low-spin η^1-peroxoiron(III) adduct.

Reactivity of the H_2O_2 adduct of complex 2: In order to study the reaction of the peroxoiron complex with the substrate, the complex was generated at 0 °C in CH_3CN during the reaction of **2** with ten equivalents of H_2O_2. Addition of an excess of methyl phenyl sulfide resulted in the decay of the 560 nm CT band, characteristic of the intermediate peroxoiron complex. The time-dependent decay of the band intensity could be fitted with a first-order kinetic law, with respect to the peroxoiron complex, and the k_{obs} values for different concentrations are reported in Figure 8. A saturation behavior was
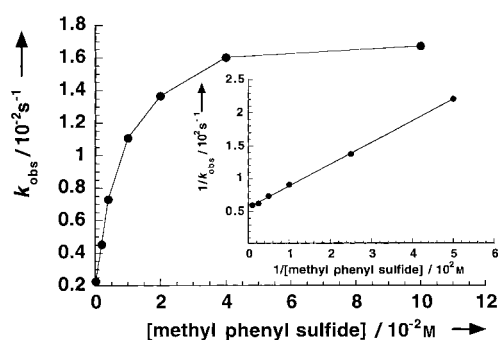

Figure 8. First-order rate constant (k_{obs}) of the decay of the complex **2**/ H_2O_2 adduct as a function of sulfide concentration at 0 °C in CH_3CN. The reaction was monitored spectrophotometrically at 600 nm, the LMCT band characteristic of the peroxoiron complex. Experimental conditions: [**2**] = 2×10^{-4} M; **2**/hydrogen peroxide: 1/10.

observed at high concentration of sulfide, supporting the notion that the substrate binds to the peroxo adduct, generating a ternary complex, before oxygen transfer. Fur-

thermore, the *ee* for the sulfoxide produced under these conditions was found to be identical to that shown in Table 1.

Discussion

Using a non-heme diiron complex with a chiral ligand we have previously demonstrated the possibility of performing catalytic enantioselective oxidation of sulfides to sulfoxides by hydrogen peroxide, thus supporting the notion that metal-based reactive oxidants are involved in this reaction.[17] In the proposed mechanism, the dinuclear structure served a key function in the stereoselective control of the reaction. Indeed, we postulated that the oxygen-atom transfer process occurred subsequent to the formation of a key intermediate ternary complex. This proceeded by the nucleophilic attack of the sulfide, bound to one Fe atom, to the electrophilic peroxide, bound to the other Fe atom, followed by H_2O release. That non-heme dinuclear Fe centers may generate reactive electrophilic peroxodiiron species has been recently supported by the demonstration that H_{peroxo}, an intermediate species formed during the reaction of the diiron(II) center of the enzyme methane monooxygenase with dioxygen, suggested to be a (μ-1,2-peroxo)diiron(III) complex, can react directly with olefins.[10] Such species have been predicted to be nucleophilic from model studies,[34] and it has been suggested that protonation occurs to form a hydroperoxide, a more electrophilic oxidant. A similar protonation of a peroxodiiron species during reaction of complex **1** with H_2O_2 has been postulated, in agreement with the observation, in this case, of a mixture of μ-peroxo- and hydroperoxodiiron(III) intermediates.[17, 33] Studies of cytochrome P450 have similarly led to the conclusion that certain substrates can be oxidized directly by a ferric hydroperoxo heme intermediate.[35]

The importance of the dinuclear structure of the iron catalyst during catalytic oxidation is now further supported by the observation reported here that the corresponding mononuclear complex has a greatly reduced ability to catalyze enantioselective oxidations by H_2O_2 in CH_3CN under argon. With all substrates, the *ee* values with mononuclear complex **2** were much lower than those with dinuclear complex **1** and in several instances *ee* = 0. Furthermore, reaction yields were much lower with complex **2** as a catalyst (Table 1).

We are aware of the fact that the mononuclear complex under study is a low-spin ferrous complex, **2**, with the proposed $[Fe(pb)_2(CH_3CN)_2]^{2+}$ structure, as supported by its spectroscopic properties and ESI-MS characterization. A ferric complex with the same structure would be a more appropriate starting material, but we failed to generate such a complex. Nevertheless, we show here that during reaction with hydrogen peroxide, complex **2** was oxidized, generating a single mononuclear peroxoiron(III) complex that is likely to be the active oxidizing species as discussed below. It thus provides the conditions for a comparison of peroxodi- and peroxomonoiron active complexes with comparable coordination spheres. Furthermore, we have strong evidence that the small amounts of the dinuclear analogue to complex **1**, present in solutions of complex **2**, were not significantly contributing to the reactions. First, no evidence for peroxo-

diiron intermediates could be obtained by Mössbauer, ESI-MS, or Raman resonance spectroscopy. Second, neither yield nor *ee* were affected by the addition of chloride, a potent inhibitor of reactions catalyzed by bipy-based diiron complexes such as complex **1**.[26]

All the spectroscopic features of the peroxoiron intermediate derived from complex **2** differ from those of each peroxodiiron adduct derived from **1** (Scheme 2).[17] UV/Vis,-
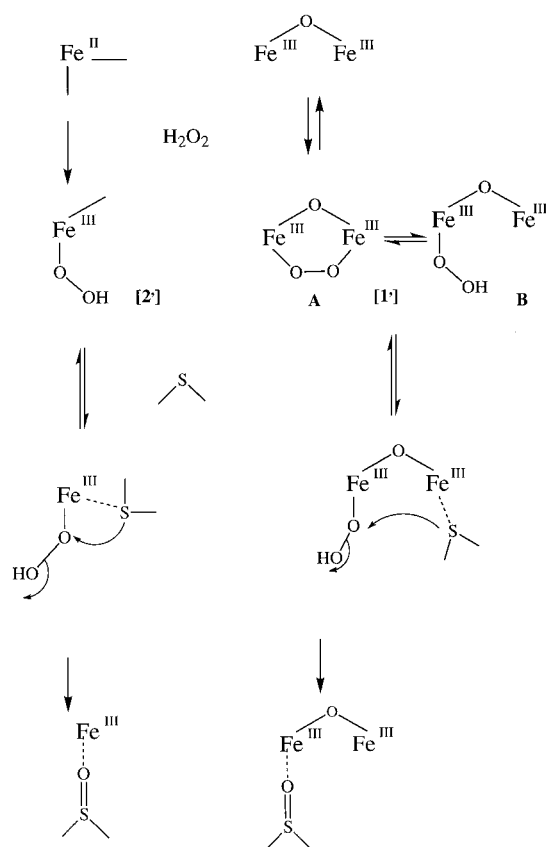
Scheme 2. Mechanistic pathways for the catalysis by complex **1** or complex **2** for the sulfide oxidation.

ESI-MS, resonance Raman, EPR, and Mössbauer spectroscopic characteristics are all consistent with a mononuclear low-spin [Fe−OOH(pb)₂] complex. This derived complex represents a new example of mononuclear Fe−OOH complexes that are postulated to be catalytic intermediates in the mechanism of mononuclear iron-dependent oxidations.

All the present results are consistent with the peroxoiron species derived from complex **2** being the active oxygen atom donor in the catalytic cycle. Detailed kinetic studies of the reaction of the peroxoiron complex with sulfide demonstrated clear saturation behavior with respect to the substrate (Figure 8). This strongly suggests that the substrate binds to the iron complex and that the ternary peroxoiron sulfide complex was a key intermediate within which an intramolecular oxo transfer takes place, as in the case of the diiron complex (Scheme 2). This was consistent with the saturation behavior of the initial rate constant of sulfoxide formation with respect to both sulfide and hydrogen peroxide concentrations (Figure 3). Thus, reactions dependent on complexes **1** and **2** are

likely to proceed similarly, with the intermediate formation of a ternary complex and reaction of the iron-bound substrate with the Fe−OOH moiety. However, only with complex **1** were the reaction kinetics correlated to the σ_p Hammet parameters, indicating that both systems have different rate-limiting steps. The difference is that the substrates bind to the single iron in reactions dependent on complex **2**, whereas they are separated, one to the first iron and the other to the second iron, in those dependent on complex **1**.

It is difficult to explain the difference between the two systems in terms of their enantioselectivity on the basis of the differences between the active ternary intermediates structures postulated in Scheme 2. Since all of the active hydroperoxo species published so far are low-spin,[22] the electrophilicity of the peroxo ligand should be comparable in both complexes. The main difference between mono and dinuclear complexes resides in the presence of the second iron site in the **1**/H₂O₂ adduct, which is suggested to play the role of the substrate binding site. Its Lewis acidity is larger than that of the low-spin ferric iron in the **2**/H₂O₂ adduct allowing a more efficient control (binding) of the substrate. Consequently, the contribution of the intramolecular oxygen-transfer pathway, within a ternary peroxoiron sulfide complex, is likely to be larger with respect to the intermolecular one, between a free sulfide and the peroxoiron intermediate, in the case of complex **1** than in the case of complex **2**. This intramolecular pathway is supposed to be more enantioselective than the intermolecular one, thus explaining the differences in enantioselectivity between the two systems.

Conclusion

This study confirms that, at least in the case of the oxidation of sulfides, non-heme peroxoiron species have the potential to directly transfer an oxygen atom to the substrates. However, there are remarkably large differences between di- and mononuclear complexes, even with comparable iron coordination environment, both in terms of efficiency and selectivity. It is thus tempting to suggest that the dinuclear structure provides the set up for a synergistic effect of the two iron sites, allowing a reaction, within the coordination sphere, between the peroxo group on one site and the sulfide on the second site.

Acknowledgement

[1] a) D. M. Kurtz, Jr., *J. Biol. Inorg. Chem.* **1997**, *2*, 159; b) P. Nordlund, H. Eklund, *Curr. Opin. Struct. Biol.* **1995**, *5*, 758.

[2] a) B. J. Wallar, J. D. Lipscomb, *Chem. Rev.* **1996**, *96*, 2625; b) M. P. Woodland, H. Dalton, *J. Biol. Chem.* **1984**, *259*, 53; c) A. C. Rosenzweig, C. A. Frederick, S. J. Lippard, P. Nordlund, *Nature* **1993**, *366*, 537.

[3] J. Green, H. Dalton, *J. Biol. Chem.* **1989**, *264*, 17698.

[4] K. K. Andersson, W. A. Froland, S.-K. Lee, J. D. Lipscomb, *New J. Chem.* **1991**, *15*, 411.

[5] a) L. M. Newman, L. P. Wackett, *Biochemistry* **1995**, *34*, 14066; b) J. D. Pikus, J. M. Studts, C. Achim, K. E. Kauffmann, E. Münck, R. J. Steffan, K. McClay, B. G. Fox, *Biochemistry* **1996**, *35*, 9106.

[6] J. Shanklin, E. Whittle, B. G. Fox, *Biochemistry* **1994**, *33*, 12787.

[7] B. G. Fox, J. Shanklin, C. Somerville, E. Münck, *Proc. Natl. Acad. Sci. USA* **1993**, *90*, 2486.

[8] a) S.-K. Lee, J. C. Neisheim, J. D. Lipscomb, *J. Biol. Chem.* **1993**, *268*, 21569; b) K. E. Liu, A. M. Valentine, D. Qiu, D. E. Edmondson, E. H. Appelman, T. G. Spiro, S. J. Lippard, *J. Am. Chem. Soc.* **1995**, *117*, 4997.

[9] a) K. E. Liu, A. M. Valentine, D. Wang, B. H. Huynh, D. E. Edmondson, A. Salifoglou, S. J. Lippard, *J. Am. Chem. Soc.* **1995** *117*, 10174; b) S.-K. Lee, B. G. Fox, W. A. Froland, J. D. Lipscomb, E. Münck, *J. Am. Chem. Soc.* **1993**, *115*, 6450; c) L. Shu, J. C. Nesheim, K. Kauffman, E. Münck, J. D. Lipscomb, L. Que, Jr., *Science* **1997**, *275*, 515.

[10] A. M. Valentine, S. S. Stahl, S. J. Lippard, *J. Am. Chem. Soc.* **1999**, *121*, 3876.

[11] a) M. Fontecave, S. Ménage, C. Duboc-Toia, *Coord. Chem. Rev.* **1998**, *178*, 1555; b) M. Costas, K. Chen, L. Que, Jr., *Coord. Chem. Rev.* **2000**, *200*, 514.

[12] a) S. Ménage, J.-M. Vincent, C. Lambeaux, M. Fontecave, *J. Mol. Catal.* **1996**, *113*, 61, and references therein; b) J. Kim, C. Kim, R. G. Harrison, E. C. Wilkinson, L. Que, Jr., *J. Mol. Catal.* **1997**, *117*, 83, and references therein; c) R. M. Buchanan, S. Chen, J. F. Richardson, M. Bressan, L. Forti, A. Mortillo, R. H. Fish, *Inorg. Chem.* **1994**, *33*, 3208; d) M. Kodera, H. Shimakoshi, K. Kano, *Chem. Commun.* **1996**, 1737; e) V. S. Kulikova, O. N. Gritsenko, A. A. Shteinman, *Mendeleev Commun.* **1996**, 119.

[13] a) R. A. Leising, R. E. Norman, L. Que, Jr., *Inorg. Chem.* **1990**, *29*, 2555; b) C. Sheu, S. A. Richert, P. Cofré, B. Ross, A. Sobkowiak, D. T. Sawyer, *J. Am. Chem. Soc.* **1990**, *112*, 1936; c) D. H. R. Barton, S. D. Béviere, W. Chavasiri, E. Cshuai, D. Doller, W.-G. Liu, *J. Am. Chem. Soc.* **1992**, *114*, 2147; d) H. C. Tung, C. Kang, D. T. Sawyer, *J. Am. Chem. Soc.* **1992**, *114*, 3445; e) M. Lubben, E. C. Meetsma, E. C. Wilkinson, B. Feringa, L. Que, Jr., *Angew. Chem.* **1995**, *107*, 1610; *Angew. Chem. Int. Ed. Engl.* **1995**, *34*, 1512 .

[14] P. A. Mc Faul, K. U. Ingold, D. D. M. Wayner, L. Que, Jr., *J. Am. Chem. Soc.* **1997**, *119*, 10594.

[15] a) Y. Mekmouche, C. Duboc-Toia, S. Ménage, C. Lambeaux, M. Fontecave, *J. Mol. Catal. A* **2000**, *156*, 85; b) C. Kim, K. Chen, J. Kim, L. Que, Jr., *J. Am. Chem. Soc.* **1997**, *119*, 5964; c) K. Chen, L. Que, Jr., *Chem. Commun.* **1999**, 1375.

[16] P. Hayoz, A. von Zelewsky, H. Stoeckli-Evans, *J. Am. Chem. Soc.* **1993**, *115*, 5111.

[17] C. Duboc-Toia, S. Ménage, R. Y. N. Ho, L. Que, Jr., C. Lambeaux, M. Fontecave, *Inorg. Chem.* **1999**, *38*, 1261.

[18] N. Ono, H. Miyake, T. Saito, A. Kaji, *Synthesis* **1980**, 952.

[19] C. R. Johnson, J. E. Keiser, *Org. Synth.* **1996**, *46*, 78.

[20] A. X. Trautwein, E. Bill, E. L. Bominaar, H. Winkler, *Struct. Bonding* **1991**, *78*, 1.

[21] J. Kim, Y. Dong, E. Larka, L. Que, Jr. *Inorg. Chem.* **1996**, *35*, 2369.

[22] a) R. Y. N. Ho, G. Roelfes, B. L. Feringa, L. Que, Jr., *J. Am. Chem. Soc.* **1999**, *121*, 264; b) I. Bernal, I. M. Jensen, K. B. Jensen, C. J. McKenzie, H. Toflund, J. P. Tuchagues, *J. Chem. Soc. Dalton Trans.* **1995**, 3667; c) A. J. Simaan, F. Banse, P. Mialane, A. Boussac, S. Un, T. Kargar-Grisel, G. Bouchoux, J. J. Girerd, *Eur. J. Inorg. Chem.* **1999**, 993.

[23] a) M.-N. Collomb-Dunand-Sauthier, A. Deronzier, C. Duboc-Toia, M. Fontecave, K. Gorgy, J.-C. Leprêtre, S. Ménage, *J. Electroanal. Chem.* **1999**, *469*, 53; b) M.-N. Collomb, A. Deronzier, K. Gorgy, J.-C. Leprêtre, *New J. Chem.* **2000**, *24*, 455.

[24] P. Mialane, A. Nivorojkine, G. Pratviel, L. Azéma, M. Slany, F. Godde, A. Simaan, F. Banse, T. Kargar-Grisel, G. Bouchoux, J. Sainton, O. Horner, J. Guilhem, L. Tchertanova, B. Meunier, J.-J. Girerd, *Inorg. Chem.* **1999**, *38*, 1085.

[25] a) A. H. R. Al-Obaidi, K. B. Jensen, J. J. McGravey, H. Toftlund, B. Jensen, S. E. J. Bell, J. G. C. Caroll, *Inorg Chem.* **1996**, *35*, 5055; b) Y. Zang, J. Kim, Y. Dong, E. C. Wilkinson, E. H. Appelman, L. Que, Jr., *J. Am. Chem. Soc.* **1997**, *119*, 4197.

[26] S. Ménage, J. M. Vincent, C. Lambeaux, G. Chottard, A. Grand, M. Fontecave, *Inorg. Chem.* **1993**, *32*, 4766.

[27] B. F. M. Matzanke, E. Bill, C. Butzlaff, A. X. Trautwein, H. Winkler, C. Hermes, H.-F. Nolting, R. Barbieri, U. Russo, *Eur. J. Biochem.* **1992**, *207*, 747.

[28] a) W. T. Oosterhuis, G. Lang, *J. Chem. Phys.* **1969**, *50*, 1381; b) W. T. Oosterhuis, G. Lang, *Phys. Rev.* **1969**, *178*, 439.

[29] a) C. P. S. Taylor, *Biochim. Biophys. Acta* **1977**, *491*, 137; b) V. Schünemann, A. M. Raitsiminring, R. Benda, A. X. Trautwein, T. K. Shokireva, F. A. Walker, *J. Biol. Inorg. Chem.* **1999**, *4*, 708.

[30] R. M. Burger, T. A. Kent, S. B. Horwitz, E. Münck, J. Peisach, *J. Biol. Chem.* **1983**, *258*, 1559.

[31] J. Hwang, C. Krebs, B. H. Huynh, A. Edmondson, E. C. Theil, J. E. Penner-Hahn, *Science* **2000**, *287*, 122, and references therein.

[32] P. Gütlich, R. Link, A. X. Trautwein, *Mössbauer Spectroscopy in Transition Metal Chemistry*, Springer, Berlin, **1978**.

[33] The full characterization of the two peroxo adducts of complex **1** will be published elsewhere.

[34] T. C. Brunold, N. Tamura, N. Kitajima, Y. Moro-oka, E. I. Solomon, *J. Am. Chem. Soc.* **1998**, *120*, 5674.

[35] G. M. Raner, E. W. Chiang, A. D. N. Vaz, M. J. Coon, *Biochemistry* **1997**, *36*, 4895, and references therein.

[36] R. Aasa, T. Vånngard, *J. Magn. Reson.* **1975**, *19*, 308.